ELSEVIER

Biophysical Chemistry 76 (1999) 185–198

Biophysical Chemistry

Effect of transport and competition on ligand binding

C.A. Condat[a,*], P.P. Delsanto[b], E. Ruffino[b], G. Perego[b]

[a] *Department of Physics, University of Puerto Rico, Mayaguez, PR 00680, USA*
[b] *INFM-Dipartimento di Fisica, Politecnico di Torino, 10129 Torino, Italy*

Received 8 July 1998; accepted 10 August 1998

Abstract

We present a model to describe the physics of chemoreception in processes determined by competitive ligand binding. Our model describes the competition between various populations, such as ligands vs. blockers and receptors vs. decoys, in protein activation when diffusion is rate-determining. Full spatio-temporal solutions can be obtained numerically. The model structure is kept simple enough as to permit its easy generalization to describe a large subset of the manifold of possible situations occurring in nature. The power and simplicity of the proposed method are exhibited through the solution of several examples which are discussed in detail.

Keywords: Diffusion; Ligand binding; Blockers; Numerical simulation

1. Introduction

The occupation of receptors located at cell surfaces regulates a multiplicity of biological processes [1,2]. There is an enormous diversity of receptors, which may be distributed at random on the cell surface or concentrated in specific regions. The occupying ligand is an ion or a molecule that diffuses into the fluid surrounding the cell. It may originate at a distant organ, a neighboring cell, or, in the case of autocrine ligands, in the target cell itself [3]. It works as a molecular messenger that signals the triggering of a biochemical process in the cell.

The activation rate may be limited by the binding itself, by diffusion, or by a combination of both processes. For instance, acetylcholinesterase appears to be a purely diffusion-limited enzyme [4], and diffusion plays a crucial role in the calcium signaling in smooth muscle cells [5], while its role in the discharge of neurotransmitters in fast synapses is still controversial [6]. The effects of finite ligand diffusivity in the medium surrounding the receptor were studied in the pioneering work of Berg and Purcell on the physics of

* Corresponding author. Present address: FaMAF, Universidad Nacional de Córdoba, (5000) Córdoba, Argentina.

0301-4622/99/$ - see front matter
PII: S0301-4622(98)00224-5

chemoreception [7]. Later, Brownian dynamics [8] and Monte Carlo [9] simulations have been used in the numerical analysis of these problems.

Since it deals directly with occupation probabilities, our approach is different, being closer, for instance, to that of Axelrod and co-workers [10,11]. From the experimental point of view, such methods as fluorescence photobleaching recovery [12] and single-particle tracking [13] can be used to examine the kinetics of diffusion and reaction.

Cell responses can be inhibited by the (natural or exogenous) addition of molecules that interfere with the ligand binding. These molecules can be roughly classified into two groups:

1. Blockers, which may occupy the ligand binding sites, hindering the access of a true ligand to the receptor. They may also bind to other sites and cause conformational changes in the receptor that decrease the ligand binding probability. A case in point is the recently discovered blocking of HIV penetration into T cells due to the binding of certain chemokines to the CCR5 co-receptor [14]; and
2. Decoys, which are alternative receptors capable of offering binding targets that trap the ligands without triggering the desired response, thus decreasing the activation rates [3,15].

The possibility of predicting the effects of the introduction of competing species has obvious biological and pharmacological applications. It could be desirable, for example, to ascertain the characteristics of an optimum blocker or decoy. It is therefore of interest to have a model that embodies the crucial features of binding in a complex environment. We have developed a very simple model that accounts for some key factors determining activation rates in the presence of competing populations. To formulate the model, we set forward the following requirements:

1. It must describe population competition: blockers competing with ligands and acceptors competing with decoys. This interaction between the populations will be expressed through the coupling of the equations that describe the relative populations.
2. It must be capable of describing the full spatio-temporal evolution of the system. Spatial inhomogeneities may be due to the initial conditions or to the local variations generated by trapping. The model should not be confined to describing well-mixed or steady-state situations.
3. It must be kept as simple as possible, so that it may be easily interpreted and generalized. It should be adaptable with minimum work to a range as wide as possible of realistic situations.

In Section 2 we put forward our master-equation based model. The model is amenable to analytical solutions in the reaction-limited case. These solutions, which help us to better understand the numerical results obtained for the more complicated cases, are presented in Section 3. Numerical solutions for several cases of interest are discussed in Section 4. Finally, Section 5 contains the conclusions and some suggestions for future work.

2. The model

The diffusive space of the competing species is partitioned using a two-dimensional lattice, with periodic boundary conditions. Each lattice site (i,j) represents a volume element that will generally contain many diffusing particles. These particles will be assumed to be non-interacting, except when they are at a binding site, which can be occupied by a single particle. The restriction of diffusion to a two-dimensional space is not a limitation, except when it is necessary to analyze the competition between two- and three-dimensional processes [11,16], or in the case in which one of the species diffuses on the surface while the other diffuses in the bulk.

The diffusion space is populated by N species that compete in order to bind to the receptor sites. We assume that a protein is activated if and only if M receptor sites are simultaneously occupied by particles belonging to the species l (the 'ligands'). Binding by any of the other $(N-1)$

species (the 'blockers') to a single site blocks ligand binding. Of course, in a practical problem it may be required that two different ligands bind to two different sites on a protein to generate activation. Extension of our model to such cases is straightforward and will be omitted here. The protein locations will be indicated by the indices (I,J). For simplicity, we will consider that there is at most one protein at any lattice site.

We will also assume that a 'decoy' species may coexist with the proteins, and that it is able to remove ligands from the diffusion space, making them unavailable for the activation process. In this section, we assume that each decoy contains K sites that can bind one particle each. In a later section we will consider multiple binding to a single decoy site. Although this decoy may also be a protein, we restrict the usage of the name 'protein' to the species whose activation properties we are studying. The decoy locations will be indicated by the indices (R,S). More decoy types can be trivially added.

The free concentration of ligand species m, l_m, satisfies a system of coupled master-like reaction–diffusion equations,

$$\dot{l}_m(i,j;t) = \lambda_m \sum_{i'j'}^{n.n.} [l_m(i',j';t) - l_m(i,j;t)] - \dot{Q}(i,j;t), \quad (1)$$

where λ_m is the diffusion rate of species m and the sum over primed indices runs only over the nearest neighbors. The reactive part accounts for binding and unbinding at the protein and decoy receptor sites,

$$\dot{Q}(i,j;t) = \sum_{I,J} \delta_{iI}\delta_{jJ} \sum_{h=1}^{M} \dot{P}_m^{(h)}(I,J;t) + \sum_{R,S} \delta_{iR}\delta_{jS} \sum_{k=1}^{K} \dot{D}_m^{(k)}(R,S;t). \quad (2)$$

Here $P_m^{(h)}(I,J;t)$ is the probability of occupation by species m of binding site h on the protein

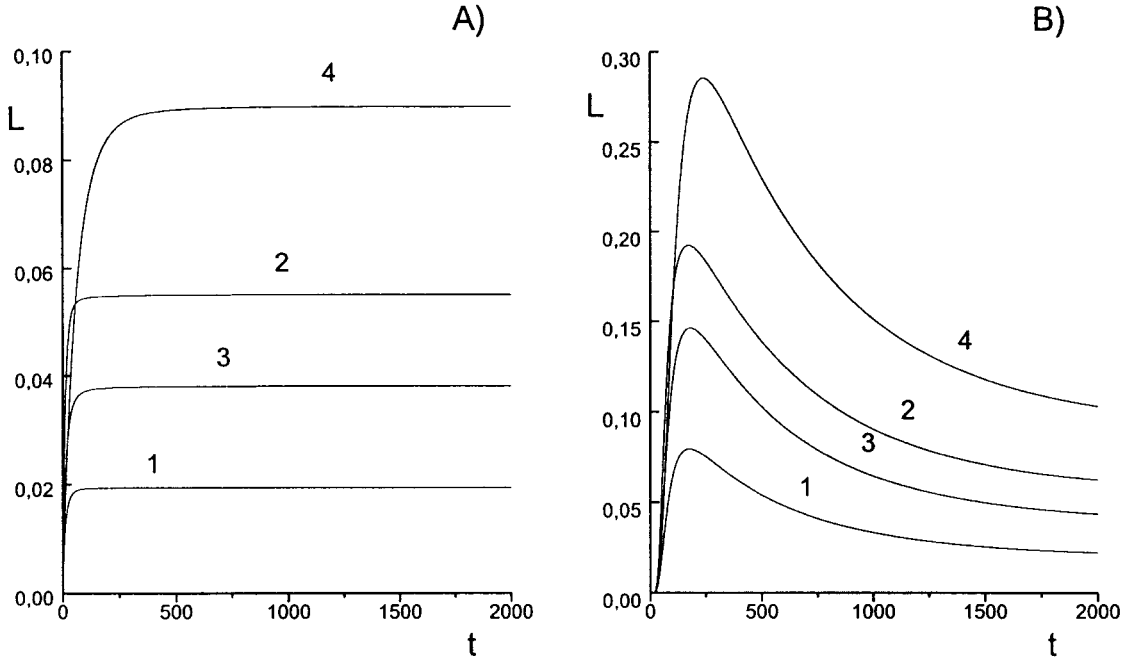

Fig. 1. Protein activation in the blocker-free case with: (a) ligands uniformly distributed at $t = 0$; (b) ligands released at a distance $r = 8\epsilon$ from the protein. For both plots $n = 50$, $\gamma = \Gamma = 0.1$, except that $n = 150$ for curves (2), $\gamma = 0.2$ for curves (3) and $\Gamma = 0.02$ for curves (4).

located at (I,J) and $D_m^{(k)}(R,S;t)$ is the probability of occupation by species m of binding site k on the decoy located at (R,S). The protein occupation probabilities satisfy the equations,

$$\dot{P}_m^{(h)}(I,J;t) = \gamma_m^{(h)}[1 - e^{-l_m(I,J;t)}] \times \left[1 - \sum_{n=1}^{N} P_n^{(h)}(I,J;t)\right] - \Gamma_m^{(h)} P_m^{(h)}(I,J;t), \quad (3)$$

with $\gamma_m^{(h)}$ and $\Gamma_m^{(h)}$ being, respectively, the absorption and desorption rates for species m at binding site h. We have included the factor $[1 - \exp(-l_m)]$ because the binding rate must be proportional to the ligand concentration at low concentrations, while it is likely to saturate at higher concentrations. The factor $[1 - \sum P]$ is added to exclude the possibility of multiple binding to a single site. The decoy occupation probabilities satisfy an analogous equation,

$$\dot{D}_m^{(k)}(R,S;t) = \delta_m^{(k)} \times [1 - e^{-l_m(R,S;t)}] \times \left[1 - \sum_{n=1}^{N} D_n^{(k)}(R,S;t)\right] - \Delta_m^{(k)} D_m^{(k)}(R,S;t). \quad (4)$$

Here $\delta_m^{(k)}$ and $\Delta_m^{(k)}$ are, respectively, the absorption and desorption rates for species m at decoy binding site k. The initial conditions will depend on the particular problem under consideration. At the start of the binding process the ligands and blockers can be uniformly distributed or can be injected into one or more specific locations. Additionally, we could have a situation in which there is a continuous input of one or more of the involved molecules.

We are neglecting correlations between different binding sites. Sometimes, binding to one site will cause a conformational modification that will affect binding to a different site. If this effect is present, a term including the intersite coupling should be introduced into the model. This should

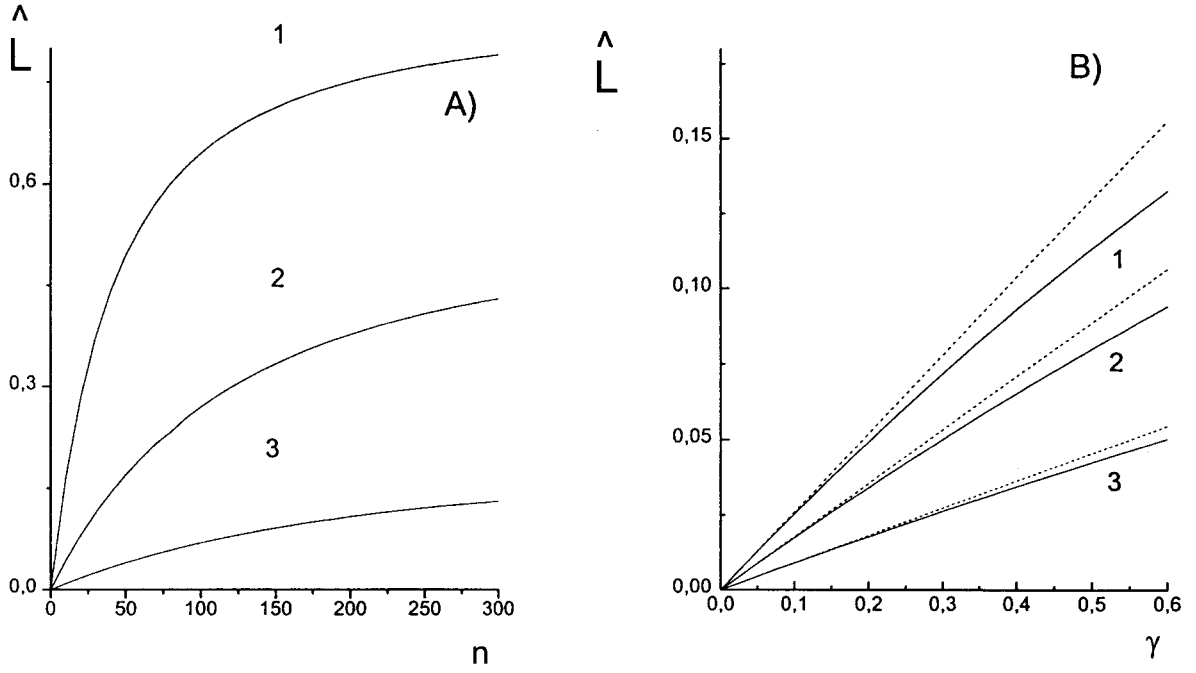

Fig. 2. Non-linearity of peak activation $\hat{L} = L(T_m)$ vs. ligand number n for three different cases: (1) $\gamma = 0.5$, $\Gamma = 0.1$; (2) $\gamma = 0.5$, $\Gamma = 0.5$; (3) $\gamma = 0.1$, $\Gamma = 0.5$. (b) Non-linearity of $\hat{L}$ vs. binding rate γ for (1) $n = 30$, (2) $n = 20$, (3) $n = 10$. The dashed lines represent the corresponding linear approximations.

be done on a case-by-case basis and we omit all further discussions here. Since in our approach the binding sites are considered independent, the probability of activation by the ligand species m for the protein located at (I,J) is given by

$$A(I,J;t) = \prod_{h=1}^{M} P_m^{(h)}(I,J;t). \quad (5)$$

To write this equation it was assumed that the active state (e.g. a channel that is open) persists while all the receptors are occupied by ligands and ceases when one is released. Other possibilities can be considered; for example, a reaction may be triggered as soon as all receptors in the protein are occupied, and whatever happens later may then become irrelevant. Eq. (5) should be suitably modified to account for the peculiarities of the problem.

3. Analytical results

3.1. The one ligand, one blocker problem

In general, the set of Eqs. (1)–(4) can only be solved numerically. However, we can find analytical solutions in some simple cases, e.g. when activation is reaction-limited; these solutions help us to understand the numerical results obtained for more complex cases.

We consider a decoy-free problem, in which we have a competition only between a ligand species ($m = 1$) and a blocker species ($m = 2$). For simplicity, we also take $M = 1$. If the diffusivities are high enough, binding will be reaction-limited. We can then assume that by a certain time T_1 the molecular concentrations in the protein neighborhood will have reached approximately their equilibrium values $l_{m,eq}$. We also consider a single protein at a time and eliminate the indices (I,J). Calling $L = P_1$, $B = P_2$, $l_{eq} = l_{1,eq}$, $b_{eq} = l_{2,eq}$, $\gamma = \gamma_1^{(1)}$, $\Gamma = \Gamma_1^{(1)}$, $\tilde{\gamma} = \gamma_2^{(1)}$, and $\tilde{\Gamma} = \Gamma_2^{(1)}$, and writing $a = [1 - \exp(-l_{eq})]$ and $\tilde{a} = [1 - \exp(-b_{eq})]$, we are left with the equations

$$\dot{L}(t) = \gamma a[1 - L(t) - B(t)] - \Gamma L(t) \quad (6)$$

$$\dot{B}(t) = \tilde{\gamma}\tilde{a}[1 - L(t) - B(t)] - \tilde{\Gamma} B(t) \quad (7)$$

These equations can be combined to obtain a single inhomogeneous differential equation for $L(t)$,

$$\ddot{L}(t) + \left(\Gamma + \tilde{\Gamma} + \gamma a + \tilde{\gamma}\tilde{a}\right)\dot{L}(t) + \left(\Gamma\tilde{\Gamma} + a\gamma\tilde{\Gamma} + \tilde{a}\tilde{\gamma}\Gamma\right)L(t) = a\gamma\tilde{\Gamma}. \quad (8)$$

The solution to this equation has the form,

$$L(t) = L_{eq} + A_1\exp(-\theta_+ t) + A_2\exp(-\theta_- t), \quad (9)$$

where it is easy to find L_{eq}, θ_+, and θ_- in terms of the model parameters. Both θ_+ and θ_- are ≥ 0. We only give here L_{eq}, the equilibrium concentration of the bound ligand:

$$L_{eq} = \frac{a\gamma\tilde{\Gamma}}{\Gamma\tilde{\Gamma} + a\gamma\tilde{\Gamma} + \tilde{a}\tilde{\gamma}\Gamma}. \quad (10)$$

We see that $L_{eq} = 1$ if $\Gamma = 0$ (i.e. if ligand binding is irreversible) and $L_{eq} = 0$ if $\tilde{\Gamma} = 0$ (i.e. if blocker

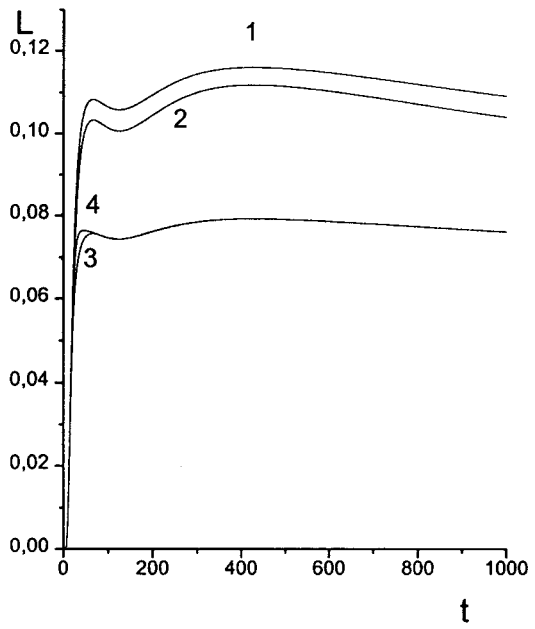

Fig. 3. Effect of blockers on protein activation for different sets of parameters. (1) $\tilde{\gamma} = 0.1$, $\tilde{\Gamma} = 0.5$; (2) $\tilde{\gamma} = 0.1$, $\tilde{\Gamma} = 0.5$ (but with a different number $\tilde{n}$ of blockers, as explained in the text); (3) $\tilde{\gamma} = 0.5$, $\tilde{\Gamma} = 0.5$; (4) $\tilde{\gamma} = 0.1$, $\tilde{\Gamma} = 0.1$.

binding is irreversible). The protein activation rate in this case is simply given by $A(t) = L(t)$. The constants A_1 and A_2 in Eq. (9) can be found using the initial conditions. For instance, if the binding site is known to be free at $t = 0$, the initial conditions are $L(0) = B(0) = 0$.

From Eq. (10) we also see that it may well be useless to add blockers beyond a certain 'saturation' value. In fact, if the blocker concentration is very high, $\tilde{a} \approx 1$ and the equilibrium activation saturates at the value $A_s = (1 + \Gamma/a\gamma + \tilde{\gamma}\Gamma/a\gamma\tilde{\Gamma})^{-1}\}$.

The blocker-free limit can be obtained by taking $\tilde{\gamma} = 0$. Then,

$$L_{eq} = \frac{a\gamma}{\Gamma + a\gamma}. \tag{11}$$

In this case, the time-dependence of the bound ligand concentration is given by,

$$L(t) = \frac{a\gamma}{\Gamma + a\gamma}[1 - e^{-(\gamma a + \Gamma)t}]. \tag{12}$$

3.2. The one protein, one decoy problem

We now consider a blockers-free case, in which we have competition between one protein and one decoy. Both species can absorb ligands, but only the protein can be activated, leading to biological processes. In this section we discuss a 'protein-like' decoy, i.e. a decoy whose occupation probability satisfies Eq. (4). Relating the probability $l(t)$ that the ligands remain free and the probabilities $L(t)$ and $D(t)$ that the ligands are bounded to the protein and to the decoy, respectively, we find

$$\dot{L}(t) = \gamma a l(t) - \Gamma L(t), \tag{13}$$

$$\dot{D}(t) = \gamma_D a l(t) - \Gamma_D D(t), \tag{14}$$

and

$$\dot{l}(t) = \Gamma L(t) + \Gamma_D D(t) - (\gamma + \gamma_D) a l(t). \tag{15}$$

Here γ_D and Γ_D are, respectively, the binding and unbinding rates at the decoy. From Eqs. (13),(14), and assuming ligand number conservation, we can easily obtain the equilibrium activation,

$$A_{eq} = L_{eq} = \frac{1}{1 + \Gamma/a\gamma + (\Gamma\gamma_D)/(\gamma\Gamma_D)}. \tag{16}$$

This equation shows that decoys are effective if $(\Gamma\gamma_D)/(\gamma\Gamma_D) \gg 1$.

3.3. Multiple-trapping decoys

As mentioned in Section 2, several decoy types can be considered. Here we briefly discuss two kinds of decoys that are capable of simultaneous multiple ligand trapping. We will call them 'tank-like' and 'macrophage-like' decoys. A tank-like decoy acts as a molecular reservoir, i.e. it can capture ligands with a rate that depends on how much it is already occupied, while its ligand release rate Γ_D is small and constant. Macrophage-like decoys can accept ligands as tank-like decoys but the unbinding rate Γ_D becomes active starting from a certain time t_R, which can be defined by the equation $D(t_R) = \tilde{D}$, where $\tilde{D}$ is the decoy occupation at which binding becomes reversible. Then we can write the following equation for the macrophage-like decoy occupation probability,

$$\dot{D}(t) = \gamma_D l_D(t) e^{-h D(t)} - \Gamma_D(t) D(t), \tag{17}$$

where h is a saturation constant and l_D is the free ligand occupation probability at the decoy location. The time-dependent release rate Γ_D is given by

$$\Gamma_D(t) = \Gamma_0[1 - e^{-k(t - t_R)}]\theta(t - t_R). \tag{18}$$

Here $\theta(x)$ is Heaviside's step function and k controls the release speed. For tank-like decoys we simply take $\Gamma_D(t) = \Gamma_0$ in Eq. (17). The equilibrium decoy occupation D_e, is always given by the solution to the transcendental equation,

$$D_e = (\gamma_D/\Gamma_0) l_e e^{-h D_e}. \tag{19}$$

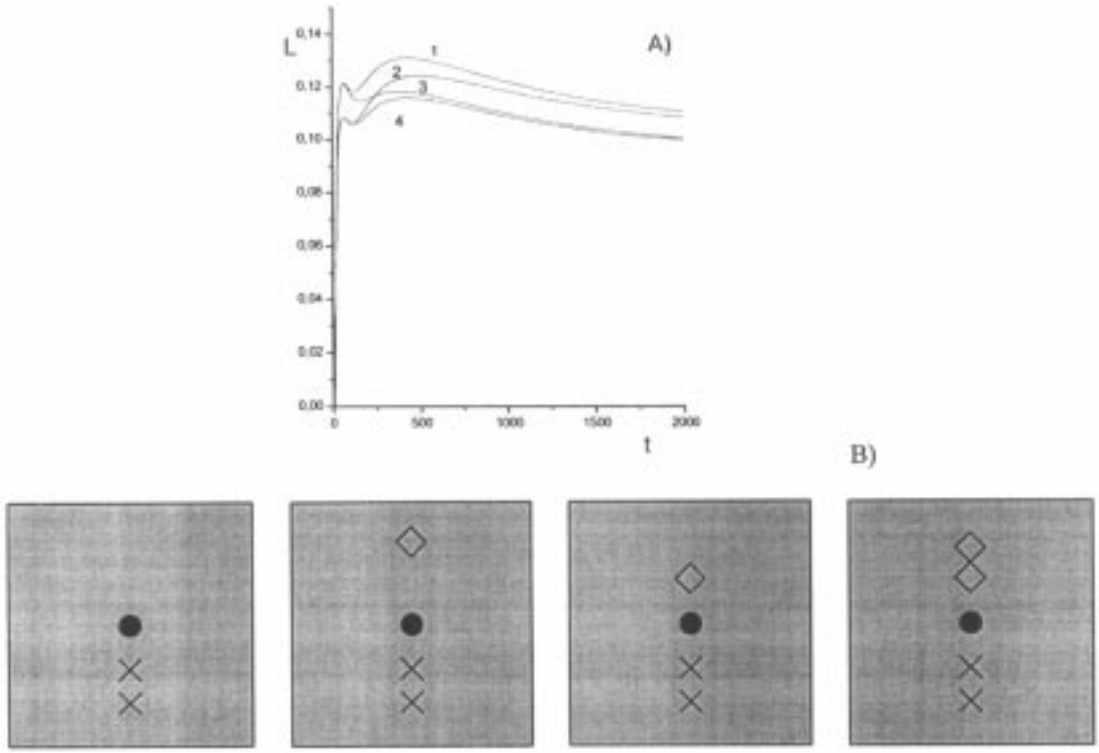

Fig. 4. (a) Influence of the initial spatial distribution of blockers and ligands on the protein activation rates. The various cases are shown in (b), where full dots, crosses and diamonds represent, respectively, the locations of the protein and the ligand and blocker input sites.

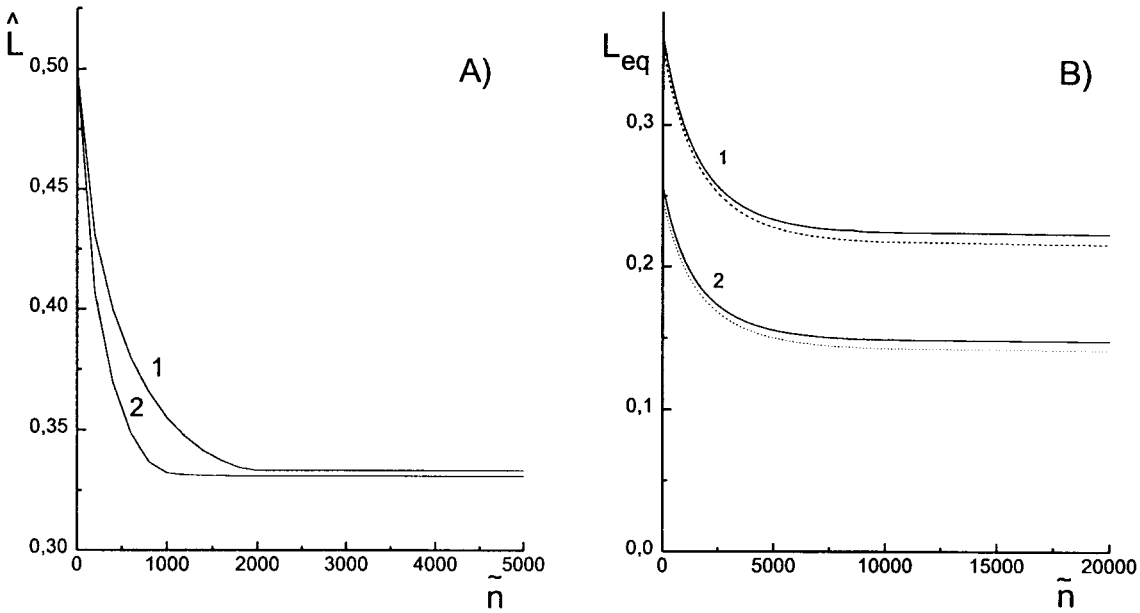

Fig. 5. Protein activation as a function of $\tilde{n}$ (a) at the peak, (b) asymptotic value. The parameters are $\gamma = \tilde{\gamma} = \Gamma = \tilde{\Gamma} = 0.1$ and (1) $n = 2000$, (2) $n = 1000$. Dashed and dotted lines represent the corresponding analytical evaluations.

4. Numerical results

The numerical technique, which we apply to the solution of the general problem outlined in Section 2, is based on the Local Interaction Simulation Approach (LISA). The method LISA is particularly suitable for parallel processing and has been successfully applied to several problems of diffusion, absorption, growth and wave propagation, see e.g. [17–20]. After a time discretization (space has been already discretized in Section 2) we obtain from Eq. (3)

$$P_m^{(h)}(t+\tau) = P_m^{(h)}(t) + \tau\left\{\gamma_m^{(h)}[1-e^{I_m(t)}] \times\left[1-\sum_{n=1}^{N} P_n^{(h)}(t)\right] - \Gamma_m^{(h)} P_m^{(h)}(t)\right\} \quad (20)$$

where we have omitted the (I, J) variables and introduced the time step τ.

As a first application of our model, we investigate how an inhomogeneity in the initial ligand distribution affects the activation rate. Fig. 1 shows the results obtained when no blockers are present and n ligands are: (a) uniformly distributed over the diffusion space at $t = 0$; and (b) initially injected at a point located at a distance $r = 8\epsilon$ (ϵ is the space discretization step) from the protein. In the former case, since the initial distribution is already uniform, after some time needed for the ligands to activate the protein, a steady state is reached. In the latter case the ligands start diffusing through the whole lattice, reaching a maximum concentration in the protein site at a certain time t_m. Shortly afterwards, at a time T_m, the corresponding maximum is obtained. At later times the protein activation decreases due to outgoing diffusion, which brings the ligands concentration at the protein site to an asymptotic value, as in case (a). The time t_m may

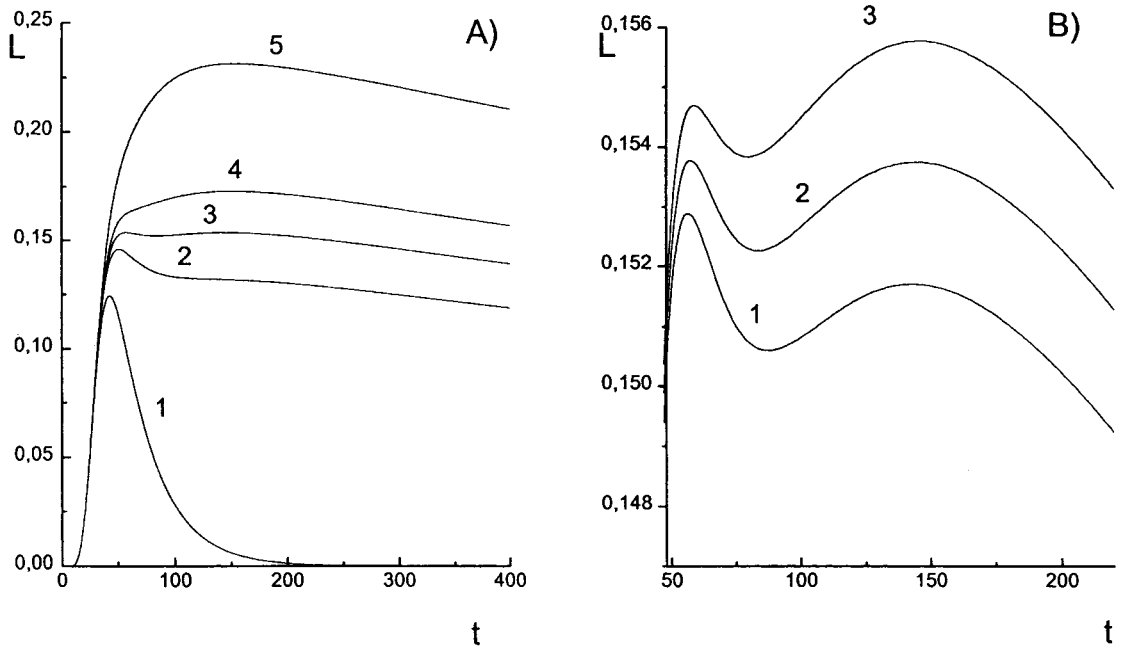

Fig. 6. Effect of blockers on the protein activation for different values of $\tilde{\Gamma}$. a: (1) $\tilde{\Gamma} = 0$, (2) $\tilde{\Gamma} = 0.04$, (3) $\tilde{\Gamma} = 0.05004$, (4) $\tilde{\Gamma} = 0.06$, (5) $\tilde{\Gamma} = 0.1$; b: (1) $\tilde{\Gamma} = 0.04904$, (2) $\tilde{\Gamma} = 0.05004$, (3) $\tilde{\Gamma} = 0.05104$. The other parameters are $n = 500$, $\tilde{n} = 1000$, $\gamma = \Gamma = 0.1$, and $\tilde{\gamma} = 0.2$.

be calculated from the solution of the diffusion equation for cylindrical symmetry [21]: $t_m = r^2/4\lambda$; for the parameters used in Fig. 1 $t_m = 160$ a.u. The time $T_m > t_m$ depends of course on the interplay of the binding–unbinding rates γ and Γ.

The protein activation is obviously an increasing function of n: for small ligand concentrations this function should be linear. In fact (see Fig. 2a), the peak activation $\hat{L} = L(T_m)$ grows linearly at first, but then saturates. $\hat{L}$ is maximized by choosing values of γ (Γ) as large (small) as possible. Increasing γ the non-linear behavior of $\hat{L}$ starts later for smaller values of n (see Fig. 2b).

The effect of the introduction of one blocker species is analyzed in Figs. 3–7. For these figures we choose the diffusivities of both ligands and blockers to be 0.1. In Fig. 3, 250 ligands and 250 blockers are injected at a distance $r = 5\epsilon$ from the protein and, in addition, 2000 ligands and 2000 blockers are also injected at a distance $r = 15\epsilon$ for all curves, except that in curve (2) the number of injected blockers is five times larger. The other parameters are $\gamma = \tilde{\gamma} = 0.1$, $\Gamma = \tilde{\Gamma} = 0.5$, except that $\tilde{\gamma} = 0.5$ in curve (3) and $\tilde{\Gamma} = 0.1$ in curve (4). Our particular selection of parameters gives rise to two activation maxima in curves (1) and (2), while curves (3) and (4) are flatter due to the increasing (decreasing) of the blockers binding (unbinding) rates $\tilde{\gamma}$ ($\tilde{\Gamma}$). Curve (2), obtained by a fivefold increase of the number of blockers in both bursts, follows closely curve (1), except at the very beginning, since there is almost saturation of blockers in both cases. Likewise a fivefold increase of $\tilde{\gamma}$ or decrease of $\tilde{\Gamma}$ have almost the same effect, i.e. a strong reduction of the protein activation, with a slight anticipation if the effect is due to an increase of the binding, rather than to a decrease of the unbinding. The explicit dependence on the initial location of the blockers bursts is shown in Fig. 4.

The dependence of the peak ($\hat{L}$) and equilibrium (L_{eq}) activations on the number of injected blockers $\tilde{n}$ is shown in Fig. 5. In both cases the curves are monotonically decreasing functions of $\tilde{n}$, but saturation occurs when $\tilde{n}$ is sufficiently large, as predicted by Eq. (10). In fact, l_{eq} (b_{eq}) becomes asymptotically equal to the number of

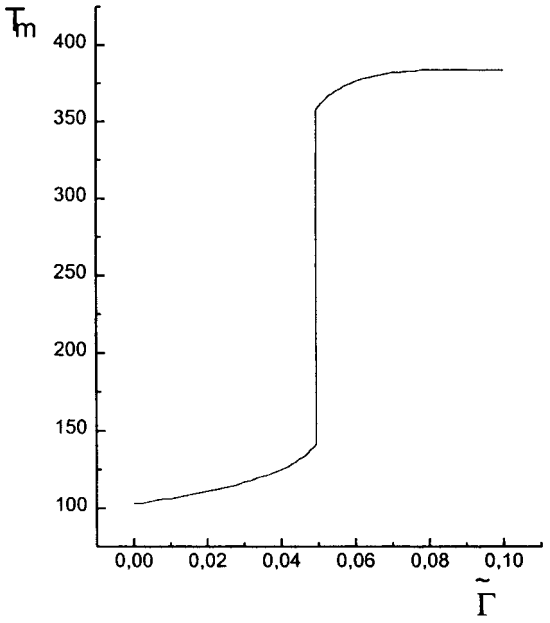

Fig. 7. Effect of $\tilde{\Gamma}$ on the maximum activation time. The vertical step marks the transition from a predominance of the first peak to a predominance of the second one.

ligands (blockers) divided by the number of the lattice sites (50^2). In addition, Fig. 5a shows the analytical evaluations (see Section 3.1) for $\hat{L}$ in both cases ($n = 2000$ and $n = 1000$).

In Fig. 6a we analyze the effect of varying the blocker release rate $\tilde{\Gamma}$. In all cases L reaches a maximum and then decreases slowly in time, except when $\tilde{\Gamma}$ is very small, in which case the peak is well pronounced. This suggests that the best way to optimize blockers efficiency is to reduce their release rate. Another feature in Fig. 6a deserves further discussion. When $\tilde{\Gamma}$ increases starting from zero, the position of the peak shifts slowly towards longer times. However, when $\tilde{\Gamma}$ is close to 0.05, a second peak appears at a much later time. At $\tilde{\Gamma} = 0.05004$ both peaks have the same height. By further increasing $\tilde{\Gamma}$ one notices that the second peak becomes the dominant one, up to when the first disappears altogether.

This effect is shown in more detail in Fig. 6b, where for very small variations of $\tilde{\Gamma}$ the first peak is higher [curve (1)], equal [curve (2)] and finally smaller [curve (3)] than the second one. Fig. 7

shows the time of maximum activation as a function of the blockers release rate. This surprising behavior can be explained in terms of lattice diffusion dynamics. In fact, both ligands and blockers arrive at the same time at the protein site, but the different absorption and desorption rates lead to a strong competition. The first peak is reached when the concentrations of ligands and blockers in the protein site have not yet arrived at their maximum value and blockers, which have a smaller release rate, prevail. Then, when the ligands concentration in the protein site reaches the maximum value, they prevail and thus cause a second activation peak. Therefore the vertical step in Fig. 7 corresponds to a region in which the time of maximum activation is extremely sensitive to very small changes in the blockers release rate.

Next we consider the problem of protein activation when there are ligand-absorbing decoys and, as a result, the protein activation is reduced. Asymptotically the activation will reach the same equilibrium value for different initial positions of the decoy [see Eq. (16)], but at finite times the relative locations of the protein, decoy, and ligand source sites are important; by inspecting Fig. 8a one sees that the decoy is most effective when it is close to the protein and along the line joining the protein to the ligand. In this case, the decoy

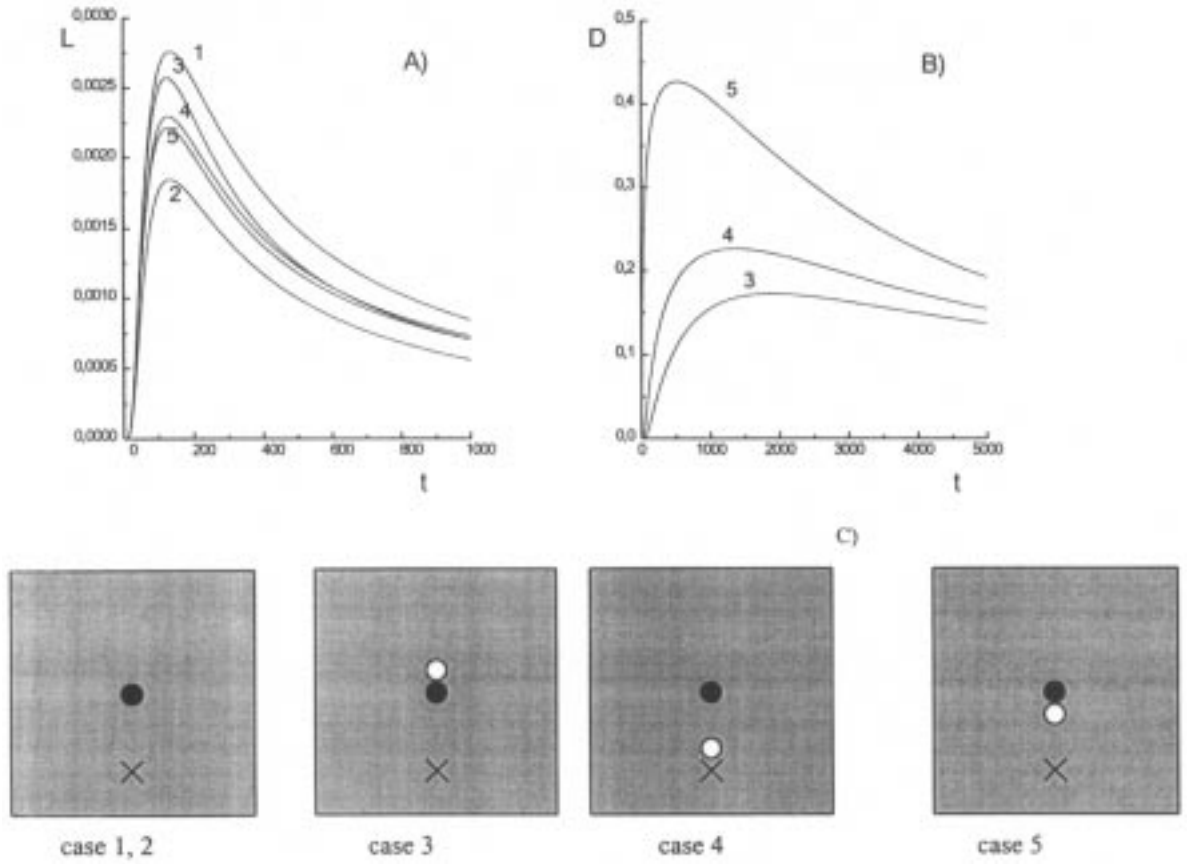

Fig. 8. Effect of the relative positions of a protein-like decoy with respect to the protein and ligands site: (a) on the protein activation; (b) on the ligands concentration in the decoy. The parameters are: $n = 3$ (except $n = 2$ in case 2), $\gamma = 0.1$, $\Gamma = 0.5$, $\gamma_D = 0.1$, $\Gamma_D = 0.001$, $r = 5\epsilon$; (c) pictorial representation of the relative positions of ligand source (cross), decoy (open circle) and protein (full dot).

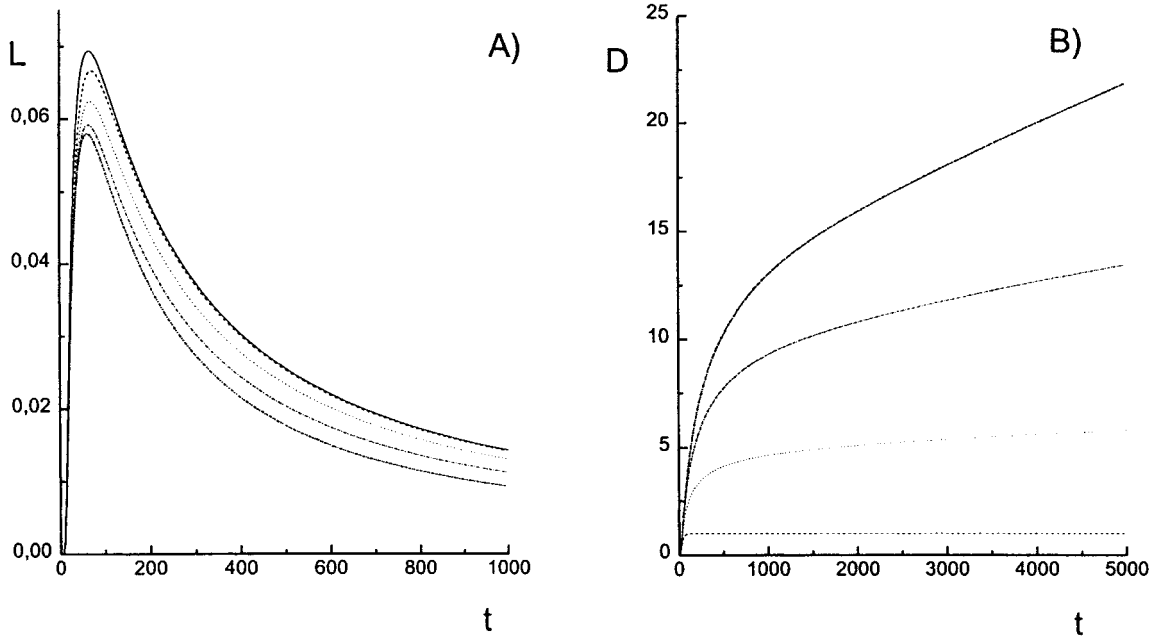

Fig. 9. (a) Effect of a tank-like decoy on protein activation. (b) The tank-like decoy occupation. In (a) the curves represent from top to bottom the cases of no decoy, protein-like (single occupancy) decoy, and tank-like decoys with $h = 0.5$, 0.1 and 0, respectively. In (b) the corresponding curves appear in the opposite sequence. The relevant parameters are $\gamma = \gamma_D = 0.1$, $\Gamma = 0.5$, $\Gamma_D = 0.001$.

can efficiently shield the protein. This effect can be appreciated more clearly in Fig. 8b, where the decoy occupation probability is depicted. Its maximum is highest when the decoy is in between the protein and the ligands (case 5) and lowest when it is behind the protein (case 3). Relative positions are even more crucial in the case of irreversible binding.

In Fig. 9 we compare the effects of a 'tank-like' decoy, e.g. a decoy that satisfies Eq. (17) with Γ_D being constant, with those of a 'protein-like' decoy, such as described by Eq. (4) and in Section 3.2. The activation and the decoy occupation probabilities are depicted in Fig. 9a,b, respectively. From Fig. 9b we see that tank-like decoys with a low value of the saturation coefficient h are most efficient in reducing protein activation.

In Fig. 10 we compare the time evolution of the activation and decoy occupation probabilities for 'macrophage-like' and 'tank-like' decoys. Curve (1) corresponds to a tank-like decoy with a fixed desorption rate, $\Gamma_D = 0.001$. Curves (2) and (3) correspond to a macrophage-like decoy, such as described by Eqs. (17) and (18), which starts releasing ligands at a certain time t_R, when the ligand concentration reaches a fixed threshold $\tilde{D}$ [equal to 15 for curve (2) and to 25 for curve (3)].

In Fig. 11 we present an example of activation triggered by the simultaneous occupancy of both receptors in a $M = 2$ protein. Fig. 11a depicts the no blocker case. As expected, the requirement that a second receptor be simultaneously occupied decreases the activation. It is clear from Eqs. (3) and (5) that the activation reduction depends strongly on the ratio between the two desorption rates. Thus we have the smallest activation reduction for $\Gamma_2 = 0.001 \ll \Gamma_1 = 0.1$. Similar conclusions can also be drawn from Fig. 11b, where we compare the effects of blocker inclusion in the one-receptor ($M = 1$) and two-receptor ($M = 2$) activation cases.

5. Conclusions

We have presented a versatile method to study protein activation when it is controlled by the

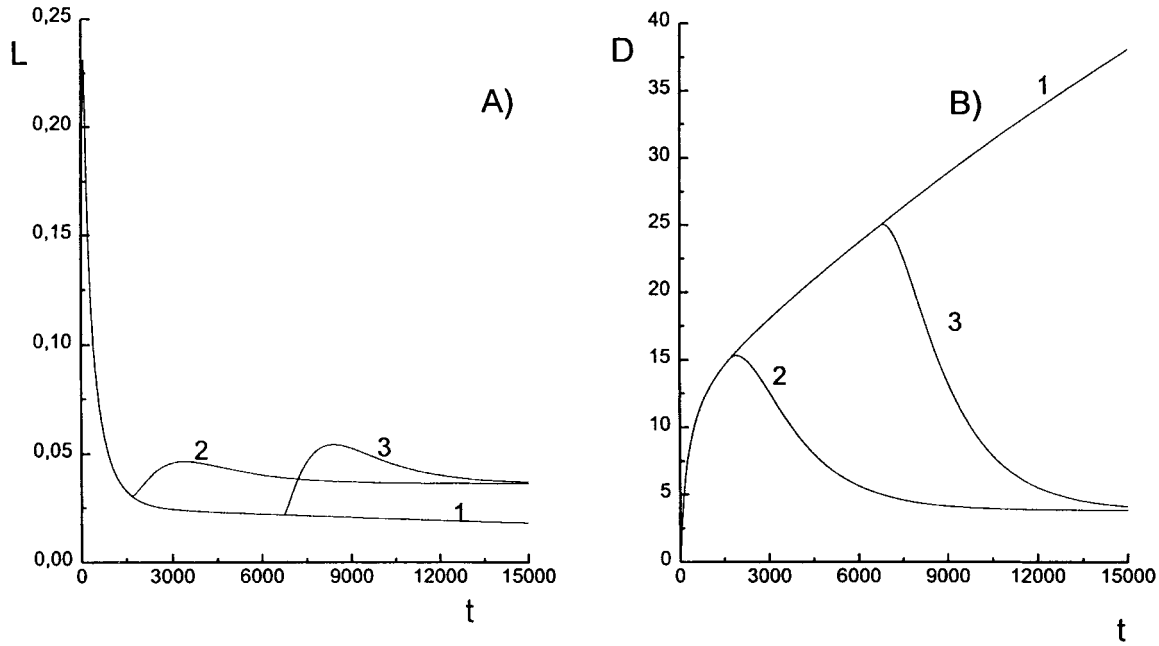

Fig. 10. (a) Effect of a macrophage-like decoy on protein activation. (b) Macrophage-like decoy occupation. Curves (2) and (3) refer to macrophage-like decoys with release thresholds $\tilde{D} = 15$ and $\tilde{D} = 25$, respectively. Curve (1) represents the case of a tank-like decoy. In all cases $h = k = 0.001$. The other parameters are the same as in Fig. 9.

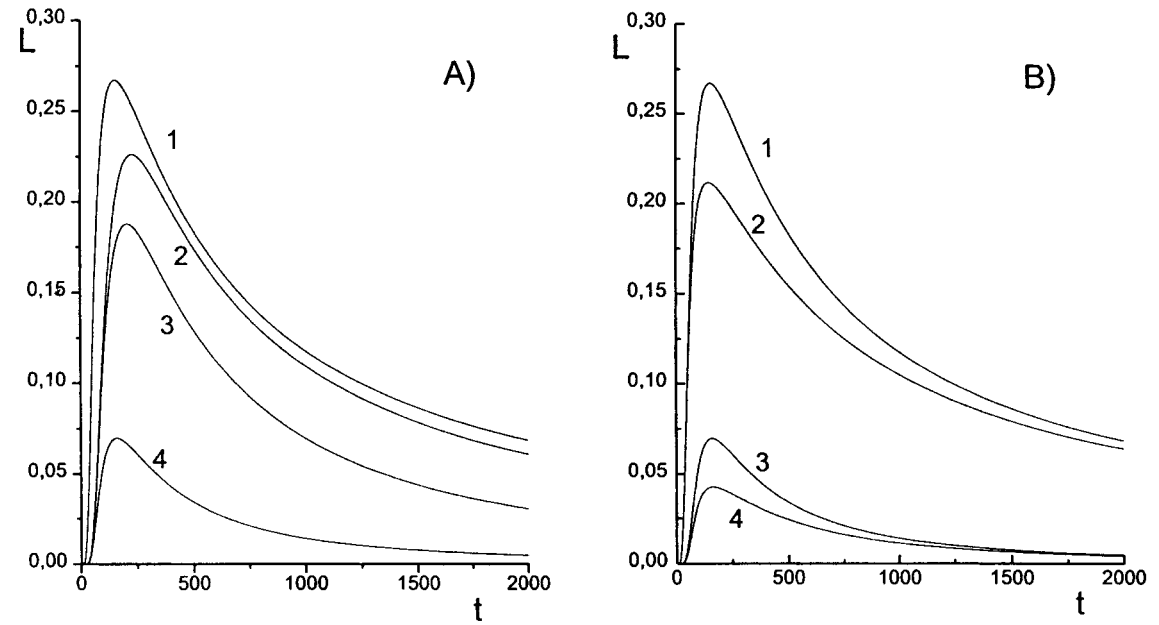

Fig. 11. Comparison between the activations of one-receptor and two-receptors protein. (a) Without blockers. Curve (1): one-receptor protein with $\gamma = \Gamma = 0.1$. Curves (2)–(4): two-receptors with $\gamma_{1,2} = 0.1$, $\Gamma_1 = 0.1$ and $\Gamma_2 = 0.001$, 0.01 and 0.1, respectively. (b) With blockers: $\gamma_{1,2} = \Gamma_{1,2} = \tilde{\gamma}_{1,2} = \tilde{\Gamma}_{1,2} = 0.1$. Curve (2): one receptor. Curve (4): two receptors. Curves (1) and (3) represent the corresponding reference (no blockers) cases.

binding of diffusing ligands. After deriving formulas that describe relatively simple situations, we have used the numerical method to investigate the effects of blockers and decoys on the activation rates. The examples show that our procedure allows a detailed prediction of the influence of competing populations in the full spatio-temporal evolution. In particular, the spatial distribution of the molecular sources often proves to be of paramount importance.

There are many applications for which our method is well-suited. In fact, it can be used to predict the efficiency of blockers and decoys as activation modifiers (interspecies competition). It can also be used to investigate intraspecies competition: this would be the case, for instance, if we consider the screening effect due to the simultaneous presence of many ligand-binding proteins in a small region. It is straightforward to extend the method presented in this paper to treat cases in which the diffusion space is not homogeneous. This occurs in the cell interior, where cytoskeleton and organelles create diffusion barriers, but it can also happen that the membrane itself is inhomogeneous [22]. The complicated geometrical constraints due to the presence of 'corrals' [23,24] are easy to model by the introduction of local changes in the corresponding master equations. Likewise, the ease with which we can add anisotropies to the jump rates permits the modelling of ligand diffusion and binding under flow conditions [25]. The method may also be applied to more general situations, such as the analysis of the relevance of flow in determining the adhesion rate of certain cancer cells to substrates [26].

Acknowledgements

This work was partially supported by the National Science Foundation through Grant No. HRD-9450342. We are also grateful to the Ministero dell'Universitá e della Ricerca Scientifica e Tecnologica (Italy) for the grant that allowed the cooperation between the Politecnico of Torino and the University of Puerto Rico. C.A. Condat is a member of CONICET, Argentina.

References

[1] R.B. Gennis, Biomembranes, Springer-Verlag, New York, 1989.
[2] D.A. Lauffenburger, J.J. Lindermann, Receptors, Oxford U. Press, New York, 1993.
[3] K.E. Forsten, D.A. Lauffenburger, Autocrine ligand binding to cell receptors. Biophys. J. 61 (1992) 518–529.
[4] J. Antosiewicz, M.K. Gilson, I.H. Lee, J.A. McCammon, Acetylcholinesterase: diffusional encounter rate constants for dumbbell model of ligand. Biophys. J. 68 (1995) 62–68.
[5] G.J. Kargacin, Calcium signaling in restricted diffusion spaces. Biophys. J. 67 (1994) 262–272.
[6] R. Khanin, H. Parnas, L. Segel, Diffusion cannot govern the discharge of neurotransmitter in fast synapses. Biophys. J. 67 (1994) 966–972.
[7] H.C. Berg, E.M. Purcell, Physics of chemoreception. Biophys. J. 20 (1977) 193–219.
[8] S.H. Northrup, Diffusion-controlled ligand binding to multiple competing cell-bound receptors. J. Phys. Chem. 92 (1988) 5847–5850.
[9] M.R. Riley, H.M. Buettner, F.J. Muzzio, S.C. Reyes, Monte Carlo simulation of diffusion and reaction in two dimensional cell structures. Biophys. J. 68 (1995) 1716–1726.
[10] D. Wang, S.-Y. Gou, D. Axelrod, Reaction rate enhancement by surface diffusion of absorbates. Biophys. Chem. 43 (1992) 117–137.
[11] D. Axelrod, M.D. Wang, Reduction-of-dimensionality kinetics at reaction-limited cell surface receptors. Biophys. J. 66 (1994) 588–600.
[12] H.V. Hsieh, N.L. Thompson, Theory for measuring bivalent surface binding kinetics using total internal reflection with fluorescence photobleaching recovery. Biophys. J. 66 (1994) 898–911.
[13] H. Qian, M.P. Sheetz, E.L. Elson, Single particle tracking. Biophys. J. 60 (1991) 910–921.
[14] G. Simmons, et al., Potent inhibition of HIV-1 infectivity in macrophages and lymphocytes by a novel CCR5 antagonist. Science 276 (1997) 276–279.
[15] K.E. Forsten, D.A. Lauffenburger, Interrupting autocrine ligand-receptor binding: comparison between receptor blockers and ligand decoys. Biophys. J. 63 (1992) 857–861.
[16] G. Adam, M. Delbrück, Structural chemistry and molecular biology, in: A. Rich, N. Davison (Eds.), W.H. Freeman, San Francisco, CA, 1968, pp. 198–210.
[17] P.P. Delsanto, R.B. Mignogna, M. Scalerandi, R.S. Schechter, Simulation of the propagation of ultrasonic pulses in complex media, in: P.P. Delsanto, A.W. Saenz (Eds.), New Perspectives on Problems in Classical and Quantum Physics, Gordon and Breach, 1997.
[18] G. Kaniadakis, P.P. Delsanto, C.A. Condat, A local interaction simulation approach to the solution of diffusion problems. Math. Comput. Modell. 17 (1993) 31–42.

[19] G. Kaniadakis, P.P. Delsanto, Simulation of desorption effects in vacuum by parallel processing. Il Nuovo Ci mento 15D (1993) 1123–1131.
[20] R.S. Schechter, H.H. Chaskelis, R.B. Mignogna, P.P. Delsanto, CM real-time parallel computation and visualization of ultrasonic pulses in solids using the connection machine. Science 265 (1994) 1188–1192.
[21] H.C. Berg, Random Walks in Biology, Princeton University Press, Princeton, 1993.
[22] A. de Beus, J. Eisinger, Modulation of lateral transport of membrane components by spatial variations in diffusivity and solubility. Biophys. J. 63 (1992) 607–615.
[23] A.P. Minton, Confinement as a determinant of macromolecular structure and reactivity. Biophys. J. 63 (1992) 1090–1100.
[24] M.J. Saxton, Single particle tracking: effects of corrals. Biophys. J. 69 (1995) 389–398.
[25] M.A. Model, G.M. Omann, Ligand-receptor interaction rates in the presence of convective mass transport. Biophys. J. 69 (1995) 1712–1720.
[26] L.A. Tempelman, D.A. Hemmer, Receptor mediated binding of IgE-sensitized rat basophilic leukemia cells to antigen-coated substrates under hydrodynamic flow. Biophys. J. 66 (1994) 1231–1243.